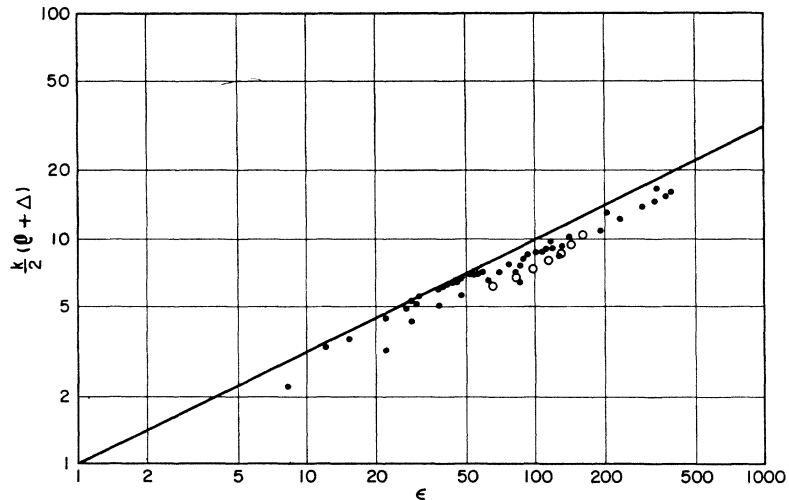


FIG. 4. Comparison of ranges of C<sup>11</sup> determined in present work (open circles) with range measurements for fission fragments (solid points) with nuclear stopping eliminated. Straight line represents theoretical curve for pure electronic stopping (see Ref. 1, Fig. 14).



line represents the theoretical curve for pure electronic stopping,  $\frac{1}{2}k\phi_0 = \epsilon^{1/2}$ . The data of the present experiment are plotted as open circles and fit well with the fission fragment range data.

Ranges of C<sup>11</sup> ions in aluminum can also be obtained from Northcliffe's integration of experimental stopping-power data for C<sup>12</sup> in aluminum.<sup>2</sup> The energy-loss measurements of 0.36 to 3.2 MeV C<sup>12</sup> ions in aluminum by Porat and Ramavataram<sup>6</sup> were included in this treatment. The resulting range-energy curve, corrected to C<sup>11</sup>, is shown in Fig. 3 as curve B. This curve includes the corrections for nuclear stopping and projected range,

<sup>6</sup> D. I. Porat and K. Ramavataram, Proc. Phys. Soc. (London) **77**, 97 (1961).

and is in essential agreement with the experimental data.

#### ACKNOWLEDGMENTS

We are grateful to Carl E. Gross and Barbara L. Jones for assisting us in various phases of this experiment and to W. G. Horath for preparing the evaporated B<sup>11</sup> target. We also wish to thank Jack R. Wallace and the crew of the Argonne tandem Van de Graaff for their cooperation. Illuminating discussions on the subject of range-energy relations were held by one of us (E. P. S.) with Professor J. Lindhard and Professor L. C. Northcliffe, and it is a pleasure to express appreciation for their help.

## Intensity Fluctuations in GaAs Laser Emission

J. A. ARMSTRONG AND ARCHIBALD W. SMITH

IBM Watson Research Center, Yorktown Heights, New York

(Received 30 April 1965)

The intensity fluctuations in the emission from various lasing and nonlasing modes of a cw GaAs laser have been measured. The measurements were made by two techniques: the coincidence-counting version of the Hanbury Brown-Twiss intensity interferometer, and the single-detector excess-photon-noise technique. The two independent methods give excellent quantitative agreement. The intensity noise in the single lasing mode was studied as the laser was taken continuously through the threshold region; this has permitted observation of the gradual change in the statistical nature of the photon noise which occurs at laser threshold. Observations have also been made of correlations between the intensity fluctuations in the emission from different modes of the laser. The experimental observations of intensity fluctuations and correlations and their dependences on injection current can be understood in terms of the response of single or of coupled van der Pol oscillators to random-noise excitation.

### I. INTRODUCTION

THE subject of noise in laser oscillators has received considerable attention in recent years. The earliest experimental work<sup>1</sup> involved the determination of the linewidth of the laser output well above

threshold. This width is due to random fluctuations in the *phase* of the oscillator. More recently experiments have been performed<sup>2-5</sup> which have detected and measured

<sup>2</sup> L. J. Prescott and A. van der Ziel, Phys. Letters **12**, 317 (1964).

<sup>3</sup> J. A. Armstrong and A. W. Smith, Phys. Rev. Letters **14**, 68 (1965).

<sup>4</sup> A. W. Smith and J. A. Armstrong, Phys. Letters **16**, 38 (1965).

<sup>5</sup> C. Freed and H. A. Haus, Appl. Phys. Letters **6**, 85 (1965).

<sup>1</sup> A. Javan, E. A. Ballik, and W. L. Bond, J. Opt. Soc. Am. **52**, 96 (1962).

ured the randomness in the *amplitude* or *intensity* of the laser light. The present paper will describe in detail the experiments we have carried out on the intensity fluctuations in the light from various modes of cw GaAs injection lasers.

Section II will describe those properties of injection lasers pertinent to the noise measurements and will also give experimental details of the two independent methods which were used to measure the intensity fluctuations. The two methods are first, the coincidence-counting version of intensity interferometry,<sup>6</sup> and second, the method of single detector, excess photon noise.<sup>7</sup> Section III presents the results of measurements of the intensity fluctuations both in the lasing mode and in the nonlasing modes. Also presented are measurements of the correlation between the intensity fluctuations in the light from different modes of the laser. In the case of the mode which lases, we present data on the intensity fluctuations as the injection current was varied from a value well below threshold to a value well above it. We have thus been able to observe the continuous change in the noise properties of the lasing mode which occurs at threshold.

In Sec. IV we present an analysis of the results in terms of the noise properties of nonlinear oscillators, using the well-known and fruitful van der Pol model oscillator.<sup>8</sup> It will be shown that all of the experimental observations on intensity fluctuations and correlations and their dependences on injection current can be understood in terms of the response of single or of coupled van der Pol oscillators to random-noise excitation. In the theoretical analysis to be given the electromagnetic field will, with a single exception,<sup>9</sup> be treated strictly classically. The work of Glauber<sup>10</sup> has shown that when a light source consists of a sufficiently large number of independent radiators (which is true of a laser below threshold), the quantum-mechanical description of the resulting total electromagnetic field is completely identifiable with a classical description. The connection between the classical and quantum descriptions of a laser above threshold is a subject of current theoretical investigation.

## II. EXPERIMENTAL DETAILS

### Injection-Laser Properties

The following facts concerning the GaAs lasers used in these experiments are pertinent. The *p-n* junctions were in the (001) plane. The lasers were small; the

<sup>6</sup> R. Q. Twiss and A. G. Little, *Australian J. Phys.* **12**, 77 (1959).

<sup>7</sup> C. T. J. Alkemade, *Physica* **25**, 1145 (1959).

<sup>8</sup> B. van der Pol, *Phil. Mag.* **3**, 65 (1927); also in *Selected Scientific Papers*, edited by H. Bremmer and C. J. Bouwkamp (North-Holland Publishing Company, Amsterdam, 1960), p. 261.

<sup>9</sup> This exception is the treatment of the random noise which drives the nonlinear oscillator. The proper expression for the spectral density of the spontaneous fluctuations in the polarization of the active medium are taken from quantum theory.

<sup>10</sup> R. J. Glauber, *Phys. Rev.* **131**, 2766 (1963).

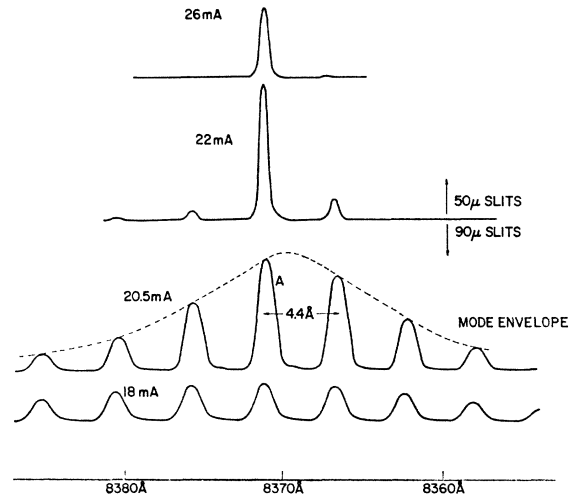


FIG. 1. Mode structure of a selected laser in the region of threshold. The intensity (vertical) scale is different at each current. The mode envelope at 20.5 mA is indicated by the dashed line. The width of all peaks is instrument limited.

active region was typically 2 by 5 by 150  $\mu$ . They had cleaved ends and etched sides; no reflective coatings were applied to the ends. The lasers were operated at  $\sim 10^\circ\text{K}$  in vacuum. At this temperature the threshold current for laser action is essentially independent of temperature; this is important since the heat dissipated in the diode varies with injection level. The diodes are driven by a stabilized dc current generator. A perhaps unique feature of injection laser oscillators is their ability to operate very stably right at threshold. This allows one to make measurements continuously throughout the regions below, at, and above threshold.

The advantages of the small size of the active region are twofold. First, the short length of the lasers means that the axial mode separation is very large compared to other lasers—about 4.4  $\text{\AA}$  in the lasers studied. This makes it very simple to isolate a single mode for study. Second, the narrow width of the lasers is very effective in discriminating against so-called off-axis modes. When the output spectra of injection lasers are examined under high resolution near threshold one often sees several (as many as five or six) families of modes,<sup>11</sup> in each of which the individual members are separated by the axial mode separation; the members of these weaker families are often called “off-axis” modes.

The lasers used in these experiments were carefully selected to find those having a single set of axial modes. The noise characteristics of a given diode, and hence its suitability for our experiments, can be assessed simply from an examination of its spectrum above and below threshold. The spectrum of a typical laser used to study intensity fluctuations is shown in Fig. 1. The envelope-narrowing characteristic of a homogeneously broadened

<sup>11</sup> P. P. Sorokin, J. D. Axe, and J. R. Lankard, *J. Appl. Phys.* **34**, 2553 (1963).

fluorescence line<sup>12</sup> is clearly exhibited by this diode. The mode marked "A" is the one which lases. A study of mode A for this diode just below threshold with a Fabry-Perot etalon of 450 Mc/sec resolution showed no structure. We believe this mode to be a true single mode at all injection currents used in these experiments; the same is true of the other nonlasing axial modes. Diodes with the simple spectrum of Fig. 1 also showed the expected far field pattern, i.e., a rectangular bright stripe with its length perpendicular to the junction plane. Finally, we note that small changes in threshold and noise behavior usually occurred after a diode was warmed to room temperature and recooled to 10°K. Thus a quantitatively consistent set of data could be obtained only by keeping the diode cold for the duration of the experiments.

### Two-Detector Technique

The coincidence-counting technique has been discussed by Hanbury Brown and Twiss<sup>13</sup> and in great detail by Twiss and Little,<sup>6</sup> and we will summarize only the major features of the method. The geometrical arrangement of the coincidence-counting experiments is shown in Fig. 2, and the block diagram of the circuitry is shown in Fig. 3. The coincidence rate  $n_c$  may be expressed as

$$n_c = 2n_1 n_2 \tau_R (1 + \rho), \quad (2.1)$$

where  $n_1$  and  $n_2$  are the single channel counting rates,  $\tau_R$  is the coincidence resolving time, and  $\rho$  is the fraction of the relative-mean-squared intensity fluctuation of the light source falling within the detector bandwidth  $(\pi\tau_R)^{-1}$ . The first term in  $n_c$  is the rate of random coincidences due to the finite resolving time. The value of  $\rho$  for a narrow-band, random-noise source of coherence

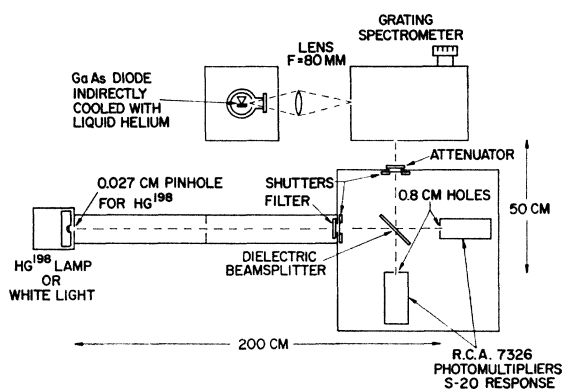


FIG. 2. Geometrical arrangement for the coincidence-counting experiments. The light from a single axial mode of the laser was isolated by the spectrometer, split into two equal beams, and allowed to fall on two identical photomultipliers. Coincidences between the output pulses of the latter were detected with the circuitry of Fig. 3. The white light and the Hg<sup>198</sup> discharge lamp were used to adjust and test the apparatus as discussed in Sec. II.

<sup>12</sup> T. H. Maiman, Phys. Rev. **123**, 1145 (1961).

<sup>13</sup> R. Hanbury Brown and R. Q. Twiss, Proc. Roy. Soc. (London) **A243**, 291 (1958).

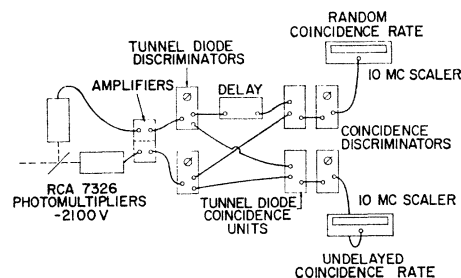


FIG. 3. Coincidence-counting circuitry. By using dual coincidence units the random and total coincidence rates were determined simultaneously. The resolving times of the two units were equalized by adjusting the coincidence discriminators.

time  $\tau_n$  is

$$\rho = \Delta_s \Delta_p \tau_n / 2\tau_R, \quad (2.2)$$

where  $\Delta_s$  is a spatial coherence factor which varies from 0 to 1, and  $\Delta_p$  is a polarization factor which varies from  $\frac{1}{2}$  for unpolarized light to 1 for linearly polarized light. This expression holds only for  $\tau_n \ll \tau_R$ , which is always the case in the work described here. In order to make  $\Delta_s$  close to one, the geometry must be chosen so that spatial coherence is obtained over the detector apertures, i.e., the central maximum of the diffraction pattern of the source at the detector must be larger than the detector aperture. The requirement may be expressed approximately as  $a_s a_d / \lambda R < 1$ , where  $a_s$  and  $a_d$  are the linear dimensions of the source and detector, respectively, and  $R$  their separation. This requirement can be easily satisfied for the diode without excessive light loss because of its high brightness. The spatial coherence factor has been evaluated by Hanbury Brown and Twiss<sup>13</sup> for the special case of a circular source and square detector. We have used their results to estimate  $\Delta_s$  for other source and detector shapes. In using the spectrometer to isolate a single mode, the diode was imaged on the entrance slit with 1:1 magnification. The image at the exit slit then forms the effective source for the experiment. The slits were adjusted to be wider than the images.

The polarization factor  $\Delta_p$  is  $\frac{1}{2}$  for unpolarized sources such as the Hg<sup>198</sup> discharge lamp and the diodes below threshold. As the injection current in the diodes is raised through threshold the light output changes continuously from the unpolarized state to a linearly polarized state.

The coincidence circuitry was of recent solid-state design,<sup>14</sup> using fast transistors and tunnel diodes. Pulses from the photomultipliers corresponding to the emission of single photoelectrons are passed by the discriminators and trigger standardized output pulses. These are fed into two coincidence units. The random coincidence rate is determined by inserting a delay in one of the inputs to one of the coincidence units. This delay is longer than the resolution time or the coherence

<sup>14</sup> Obtained from Edgerton, Germeshausen, and Grier, Inc.

time, whichever is longer. The other coincidence unit is used to determine the rate of undelayed coincidences. The fractional decrease in the coincidence rate due to the delay is called  $\rho$ .

A coincidence resolving time of about 6 nsec was used, and the single channel rates were set to be about  $5 \times 10^5$  counts/sec by attenuating the light if necessary. A typical coincidence rate was thus 3000 counts/sec. The coincidence resolving time was determined by measuring the single-channel rates on the 10 Mc/sec scalars.

The procedure used in studying intensity fluctuations was as follows. First the light from the narrow-band source being studied was allowed to fall on the photocathodes of the photomultipliers. The delayed and undelayed coincidences were counted for 1 min. Then, using a system of shutters, the narrow-band light was blocked and the light from a tungsten lamp was substituted. The intensity of the white light was adjusted to be approximately the same as that of the first source. The delayed and undelayed white light coincidences were then counted for 1 min. The white light was then blocked out, the original light reintroduced, and the cycle repeated. This pattern was repeated until the number of random coincidences recorded for each light source was about one million. This required between 10 and 15 min actual counting time. The use of the white light allowed a continuing check on the stability of the electronic circuitry. Any systematic difference between the two white-light coincidence rates can only be due to instrumental misadjustments, since the spectral density of the white light is far too low to produce any observable correlation in photon arrival times.

As a shake-down experiment we repeated the determination of the intensity fluctuations in the 4358 Å line of an air-cooled, microwave-excited, low-pressure Hg<sup>198</sup> lamp.<sup>15</sup> The geometrical coherence factor involved in this experiment was 0.44. The value of  $\rho$  obtained was  $0.010 \pm 0.002$ , which corresponds to a random-noise band width of 860 Mc/sec. This value of the linewidth is in good agreement with previous determinations.<sup>16</sup>

### Single-Detector Technique

The apparatus and procedure for measuring intensity fluctuations with the excess-noise technique are much simpler. The experimental arrangement is shown in Fig. 4. The noise voltage generated by the photocurrent in the load resistor is measured by a true rms voltmeter.<sup>17</sup> The bandwidth of the voltmeter circuit was approximately 10 Mc/sec and was held constant throughout the experiment. The desired quantity is the ratio of the noise voltage  $V_n$  measured with laser light incident on the detector to the shot noise  $V_s$  for the same average primary photocurrent  $I_{dc}$ . The shot

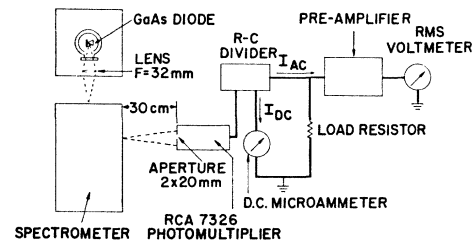


Fig. 4. Single-detector arrangement for measuring excess noise. The fluctuations in the output current of the phototube were measured with an rms voltmeter. The dc photocurrent was determined simultaneously by using an RC divider network. The low-frequency cutoff of 2 kc/sec was fixed by the divider, the high-frequency cutoff of 10 Mc/sec by the voltmeter.

noise was measured with white light incident on the detector. For a narrow-band random-noise source, the ratio of the two noise voltages is related to the coherence time  $\tau_n$  of the noise by

$$(V_n/V_s)^2 - 1 = \tau_n I_{dc} \Delta_s \Delta_p / e, \quad (2.3)$$

where  $e$  is the electronic charge. This expression holds only when the measurement frequency is less than the noise bandwidth  $1/(\pi\tau_n)$ , which is always the case for the work described here.

For the single-detector technique large values of  $I_{dc}$  are required to achieve reasonable accuracy of measurement;  $V_s^2$  must be larger than the preamplifier noise. It is necessary to make the source-detector separation as small as possible consistent with the requirement that  $\Delta_s \approx 1$ . The actual value of  $\Delta_s$  pertaining to the experiment is difficult to determine because the emitting areas of the diodes are not precisely known, but estimates indicate that it is close to one. Furthermore, it was found that the ratio  $V_n/V_s$  did not increase at values of the source-detector separation greater than the 30-cm value actually used, which is also consistent with  $\Delta_s \approx 1$ . For purposes of comparison with the coincidence measurements, the ratio  $V_n/V_s$  can be converted into an equivalent relative intensity fluctuation  $\rho_{eq}$  as follows:

$$\rho_{eq} = [(V_n/V_s)^2 - 1](e/2\tau_R I_{dc}). \quad (2.4)$$

This assumes equal values of  $\Delta_s$  and  $\Delta_p$  for both experiments. All of the single-detector measurements will be presented in terms of  $\rho_{eq}$ .

### III. EXPERIMENTAL RESULTS

Our first measurements of the intensity fluctuations in laser light were made on the single lasing mode of the diode whose spectrum is shown in Fig. 1. This mode was isolated with a 0.5-m Jarrell-Ash spectrometer of resolution sufficient to exclude all other axial modes but insufficient to in any way artificial narrow the linewidth of the lasing mode.<sup>18</sup> In Fig. 5 we show the rela-

<sup>15</sup> Obtained from Baird-Atomic, Inc.

<sup>16</sup> G. A. Rebka and R. V. Pound, *Nature* **180**, 1035 (1957). See also Ref. 6.

<sup>17</sup> Hewlett-Packard model 3400-A.

<sup>18</sup> We have made measurements of the linewidth of mode "A" both just below and well above threshold. Just below, its width is about 1300 Mc/sec; well above threshold the width is less than 50 Mc/sec (Ref. 19). Both these widths are far smaller than the resolution of the monochromator used.

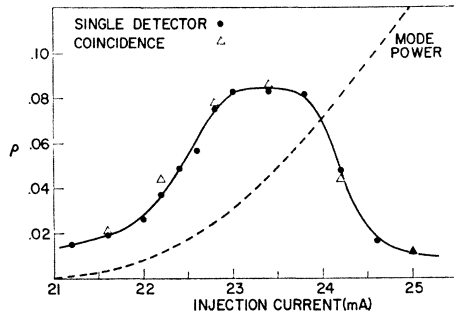


FIG. 5. The relative intensity fluctuation  $\rho$  for the lasing mode as a function of injection current  $J$ , measured by both the coincidence-counting and excess-noise techniques. The excess-noise data have been converted to an equivalent value of  $\rho$  as described in the text. The coincidence data have a constant absolute accuracy of about  $\pm 0.003$  in  $\rho$ , whereas the excess-noise data have a constant relative accuracy of about  $\pm 10\%$ . The dashed curve gives the mode power in arbitrary units.

tive intensity fluctuation  $\rho$  as a function of injection current  $J$  for the single lasing mode. Also shown is the power in mode A. Data was obtained by both the coincidence-counting technique and the single-detector excess-noise technique. The agreement between the two methods for determining the amplitude noise is excellent.

There are several features of the behavior of  $\rho$  which require explanation. Note that at injection levels near but below threshold ( $\sim 22.8$  mA in Fig. 5 and 20.5 mA in Fig. 6) the intensity fluctuations increase with increasing diode current. The fluctuations peak around threshold and thereafter decrease, falling below the limit of detectability at injection levels  $\sim 25\%$  greater than threshold. The decrease in  $\rho$  above threshold is referred to as "quieting." As will be discussed in detail later, quieting is characteristic of all good oscillators. The increase in noise below threshold can be explained as follows: Below threshold the mode emits narrow-band random noise, whose bandwidth, however, is not constant but decreases with decreasing net loss in the cavity. This decreasing net loss is of course due to the gain in the active medium. It follows from Eq. (2.2) that decreasing bandwidth (increasing  $\tau_n$ ) causes  $\rho$  to increase.

Thus if we can independently estimate the dependence of the single-mode linewidth below threshold on injection current we should be able to predict the variation of  $\rho$  with  $J$  below threshold. There are two ways of determining the linewidth. The first method is direct measurement. Figure 6 shows the variation of  $\rho$  versus  $J$  for the same laser, taken several months before the run of Fig. 5, again for the single lasing mode. The single-mode linewidth was measured with a Fabry-Perot etalon at 19.8-mA injection level; we obtained a value of  $1300 \pm 200$  Mc/sec. This linewidth corresponds to the value of  $\rho$  shown by the square and error bar in Fig. 6.

The second method involves the envelope narrowing.

The same mechanism which causes the single-mode emission to narrow is responsible for the gain narrowing of the mode envelope (fluorescence line) shown in Fig. 1. Near threshold the width  $\Delta\nu_m$  of a single mode near the center of the fluorescence line is related to the envelope width  $\Delta\nu_e$  by the expression<sup>12</sup>

$$\Delta\nu_m = \Delta\nu_{m0}(\Delta\nu_e/\Delta\nu_{e0})^2, \quad (3.1)$$

where the subscript "0" denotes an unnarrowed width. The behavior of  $\rho$  predicted from this relation, and the observed mode polarization, is shown by curve B in Fig. 6, using an estimate<sup>19</sup> of 60 000 Mc/sec for the unnarrowed mode width. Clearly the observed behavior of  $\rho$  below threshold is typical of that of a gain-narrowed, random-noise emission. It may be noted that  $\rho = 3 \times 10^{-4}$  for the unnarrowed mode, which is below the minimum detectable value of  $2 \times 10^{-3}$ .

The measurements reported so far involved intensity fluctuations in the single lasing mode. By retuning the monochromator we can study the intensity fluctuations in the nonlasing modes as well. Figure 7 shows the relative intensity fluctuations  $\rho$  for the lasing mode and for the second and third strongest, nonlasing modes. Also shown are the powers in the three modes. The second mode is seen to be much more noisy than the lasing mode at and above threshold. As will be seen, this is because the output of the nonlasing modes continues to be narrow band random noise even after the strongest mode has begun to lase and its intensity fluctuations have fallen off. The value of  $\rho$  for the third mode is smaller than for the second because the gain narrowing in the third mode is less than in the second. The eventual bending over of the  $\rho$ -versus- $J$  curve for the second mode can be understood in terms of coupling between the various modes of the laser.

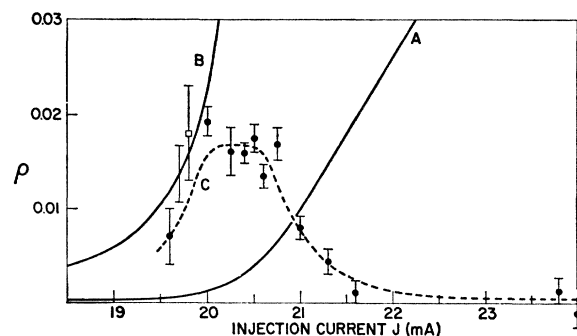


FIG. 6. The relative intensity fluctuation  $\rho$  for the lasing mode plotted against injection current  $J$  for the same maser as Fig. 5, but measured at an earlier time. The experimental points are solid circles with bars indicating the standard deviations of the counting fluctuations. Curve A shows the output power of the mode in arbitrary units. Curve B is the behavior of  $\rho$  for narrow-band noise predicted from the observed envelope narrowing. The accuracy of this curve is indicated by the error bar at  $J = 19.7$  mA. The value of  $\rho$  estimated from the measured linewidth is shown by the square. The dashed curve C is a smooth curve through the experimental points.

<sup>19</sup> J. A. Armstrong and A. W. Smith, Appl. Phys. Letters 4, 196 (1964).

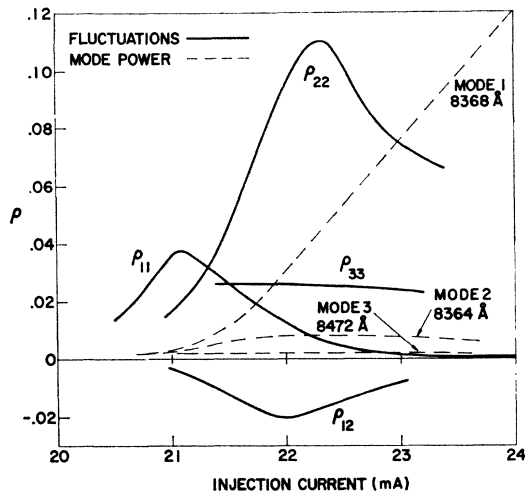


Fig. 7. Variation with injection current of the relative intensity fluctuations  $\rho_{ii}$  for the lasing and two nonlasing modes, derived from single-detector measurements. Also shown is the current dependence of the correlation  $\rho_{12}$  between the intensity fluctuations in the first (lasing) and the second (nonlasing) modes. The  $\rho_{12}$  data were taken after thermal cycling of the diode to room temperature, which caused small changes in the peak values of  $\rho_{11}$  and  $\rho_{22}$ .

Experimental observation of coupling between the intensity fluctuations in different modes was made by using the intensity interferometer as a correlator. Using two monochromators, the light from one mode was shone on one detector and the light from another mode was shone on a second detector (with the beam splitter of Fig. 2 removed). The two photomultiplier outputs were then fed to the coincidence counter, and the fractional change in the coincidence rate when a delay was inserted in one channel gave the normalized correlation between the intensity fluctuations in the two modes. Typical results are shown in Fig. 8. We show the spectrum of the laser at the injection current where the correlations were measured, the relative intensity fluctuations in each mode  $\rho_{ii}$ , and the correlations between the intensity fluctuations in pairs of modes  $\rho_{ij}$ . Note that the correlations which involve the lasing mode are negative, whereas the correlation between the two nonlasing modes is positive. The existence of both positive and negative correlations and their magnitudes can be understood in terms of the theory of coupled oscillators to be given in Sec. IV. The variation of the correlation coefficient  $\rho_{12}$  with injection level is shown by the bottom curve in Fig. 7. (Figures 7 and 8 refer to different lasers.)

#### IV. INTERPRETATION

Our discussion of the experimental results will be based on the use of van der Pol's equation to describe the behavior of a laser oscillator driven by random spontaneous emission noise. We expect intuitively that the output of a lasing mode will be a superposition of an amplitude-stabilized, coherent signal and a weaker,

random-noise signal. A nonlinear theory must be used since a linear theory is intrinsically incapable<sup>20,21</sup> of describing the effects of noise on the coherent signal and conversely the effect of the coherent signal on the noise power and the noise bandwidth.

It may be shown that van der Pol's equation is the proper nonlinear description of gas-laser oscillators. Lamb<sup>22</sup> gives a semiclassical discussion starting with Maxwell's equations for the field in the mode and including the source term which produces the field. The requirement of self-consistency, namely that the field in turn gives rise to the source, is imposed and the source is written as a function of the field, keeping terms up to third order in the field in a quantum-mechanical perturbation calculation. This procedure is familiar from the recent work in nonlinear optics.<sup>23</sup> As is also the case in nonlinear optics, the nonlinear source terms may be either in phase or out of phase with the field in the mode. For modes near the center of an homogeneously broadened fluorescent line only the out-of-phase part of the nonlinear polarization is important. In such a case Maxwell's equation for the field in the mode takes the form of van der Pol's equation. Similarly, analysis of the NMR maser clock leads to van der Pol's equation.<sup>24</sup>

The explicit demonstration of the applicability of this famous equation to the case of the GaAs injection laser has not yet been given. Certainly there are properties of injection lasers which are not reflected by this relatively simple nonlinear differential equation. It is a reasonable expectation, however, that the properties of injection lasers which are essential to their operation as oscillators are describable in terms of van der Pol's equation and in what follows we will assume that such is the case.

The problems involved in analyzing the intensity fluctuations in the output of a laser will be treated as follows. First, assuming the output to be a superposition

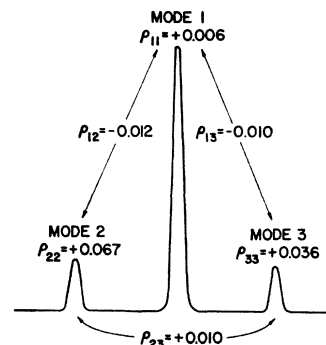


Fig. 8. The relative intensity fluctuations  $\rho_{ii}$  and the correlations  $\rho_{ij}$  between three modes (one lasing, two nonlasing) in a cw GaAs laser with the spectrum shown.

<sup>20</sup> A. Blaquièrre, *Ann. Radioelec.* **8**, 36 (1953); also **8**, 153 (1953).

<sup>21</sup> J. A. Mullen, *Proc. IRE* **48**, 1467 (1960); see also M. J. E. Golay, *Proc. IEEE* **52**, 1311 (1958).

<sup>22</sup> W. E. Lamb, Jr., *Phys. Rev.* **134**, A1429 (1964).

<sup>23</sup> J. A. Armstrong, N. Bloembergen, J. Ducuing, and P. Pershan, *Phys. Rev.* **127**, 1918 (1962).

<sup>24</sup> P. Grivet and A. Blaquièrre, in *Proceedings of the Symposium on Optical Masers* (Polytechnic Press, New York, 1963), p. 69.

of an amplitude-stabilized field and a weaker, stationary random-noise field, we will compute the value of the relative intensity fluctuation  $\rho$  to be expected. This value of  $\rho$  will turn out to depend on four parameters: the coincidence resolving time, the correlation time of the amplitude fluctuations, the power in the weak-noise field, and the power in the amplitude-stabilized field. The relationships which exist between these last three quantities will then be calculated from analysis of the response of a single van der Pol oscillator to random excitation. The final problem will be to write down the equations for several van der Pol oscillators coupled by the active medium of the laser and all driven by the random noise corresponding to spontaneous emission. Analysis of these coupled equations will provide explanations for the observed correlations between intensity fluctuations in different modes.

### Expressions for $\rho$

Assume the oscillator output to have the following form:

$$E(t) = E_0 \cos(\omega_L t + \psi_L) + e_n(t) = E_{\text{coh}}(t) + e_n(t). \quad (4.1)$$

Here  $\omega_L$  is the frequency of the laser,  $\psi_L$  is the random phase of the coherent signal, and  $e_n(t)$  represents stationary Gaussian random noise. The output noise  $e_n$  is to be distinguished clearly from the random noise which drives the laser mode; the two types of noise will have different bandwidths, powers, and different statistical properties. In what follows we assume the total field  $E(t)$  to be linearly polarized and to have constant phase across the detector apertures (i.e., we assume  $\Delta_s = \Delta_p = 1$ ).

Now expand  $e_n(t)$  in a Fourier time series over a long interval  $T \equiv \nu_0^{-1}$ .

$$E(t) = E_0 \cos(\omega_L t + \psi_L) + \sum_r h_r \cos(2\pi r \nu_0 t + \phi_r). \quad (4.2)$$

Here  $r$  is an integer, the  $h_r$  are Fourier amplitudes which have appreciable value only in the neighborhood of  $r = \omega_L / 2\pi\nu_0$ , and the  $\phi_r$  are identically distributed, independent random phases of the Fourier components.

The instantaneous power in the mode can be written

$$P(t) = P_{\text{coh}} + P_n + E_0 \sum_r h_r \times \cos[(2\pi r \nu_0 - \omega_L)t + \phi_r - \psi_L] + \frac{1}{2} \sum_{r \neq s} h_r h_s \cos[2\pi(r-s)\nu_0 t + \phi_r - \phi_s], \quad (4.3)$$

where  $P_{\text{coh}} = \frac{1}{2} E_0^2$  and  $P_n = (\frac{1}{2}) \sum_r h_r^2$ . The instantaneous output of the detector will simply be expression (4.3) multiplied by a detector efficiency  $\alpha$  expressed in pulses/sec/W.

Calculation of the expected rate of coincidences now follows very closely the derivation given in Appendix B of Ref. 13, except that there is an additional source of fluctuations due to the beats between the stabilized field and the noise field. We assume a coincidence resolving time  $\tau_R$ , and also for simplicity that each de-

tor is of equal sensitivity and that each is irradiated by the field of Eq. (4.3). The coincidence rate is

$$R = 2\tau_R (P_{\text{coh}} + P_n)^2 + \sum_{r>s} h_r^2 h_s^2 \frac{\sin[2\pi(r-s)\nu_0\tau_R]}{2\pi(r-s)\nu_0} + E_0^2 \sum_r h_r^2 \frac{\sin[2\pi(r\nu_0 - \nu_L)\tau_R]}{2\pi(r\nu_0 - \nu_L)}. \quad (4.4)$$

The first term is the random coincidence rate due to the finite resolving time; the second term was derived by Brown and Twiss and interpreted as due to bunching of photon arrival times; the third term is new and represents the intensity fluctuations due to interference between the noise and the coherent signal. Expression (4.4) can be simplified if the correlation time  $\tau_n$  of the noise power  $P_n$  is much less than or much greater than  $\tau_R$ . One changes from summation to integration by putting

$$\frac{1}{2} \sum_r h_r^2 = \int_0^\infty g^2(\nu) d\nu. \quad (4.5)$$

If  $\tau_n \ll \tau_R$ , we find

$$R = 2\tau_R (P_{\text{coh}} + P_n)^2 + \int_0^\infty g^4(\nu) d\nu + P_{\text{coh}} g^2(\nu_L). \quad (4.6)$$

The integral in (4.6) is written  $\tau_n P_n^2$  by Brown and Twiss and constitutes their definition of  $\tau_n$ . In the same spirit we write the last term as  $a\tau_n P_n P_{\text{coh}}$ ; this defines a parameter  $a$ , which clearly depends on the shape of the noise-power spectrum  $g^2(\nu)$ . This parameter has the values 1,  $\sqrt{2}$ , and 2 for rectangular, Gaussian, and Lorentzian shapes, respectively. The final expression for  $\rho$  is

$$\rho = \left( \frac{\tau_n}{2\tau_R} \right) \left( \frac{P_n^2 + aP_n P_{\text{coh}}}{(P_n + P_{\text{coh}})^2} \right). \quad (4.7)$$

Although we will not use it here, we also give the expression for  $\rho$  derived from Eq. (4.4) when  $\tau_n \gg \tau_R$ . It is

$$\rho = (P_n^2 + 2P_n P_{\text{coh}}) / (P_n + P_{\text{coh}})^2. \quad (4.8)$$

### Response of van der Pol's Oscillator to Random Noise

In order to apply expression (4.7) to the observations of  $\rho$  we must know the dependence of both  $P_n$  and  $\tau_n$  on  $P_{\text{coh}}$ . These relations can be found from analysis of the response of the nonlinear van der Pol oscillator<sup>20,21</sup> to random noise. That is, we must solve the equation

$$d^2 E / dt^2 + (r - \alpha + \gamma E^2) dE / dt + \omega_L^2 E = (\omega_L^2 / c^2) N(t). \quad (4.9)$$

In this equation  $E$  is the electric field in the cavity mode, whose bandwidth in the absence of gain is  $r$ . Apart from a frequency factor,  $(\alpha - \gamma E^2)$  is the gain of

the active medium. The field-dependent term in the gain is due to saturation; i.e., the gain of the medium decreases when an oscillation is allowed to build up.  $N(t)$  is a random function of time and represents the spontaneous fluctuations in the dipole moment of the medium<sup>25</sup> due to spontaneous emission. The time average of  $N(t)$  is zero but the average of  $N^2(t)$  is not. The spectral density of  $\langle N^2(t) \rangle_t$  is  $D(\nu)$  and contains all the information we can have about the noise driving term  $N(t)$ .

The coefficients  $\alpha$ ,  $\gamma$ , and the spectral density  $D(\nu)$  depend on the matrix element for transition from the upper to the lower level, on the fluorescence lineshape, and on the relaxation times of the states. The detailed expressions for two-level solid-state or gas systems have been given by Lamb<sup>22</sup> (for  $\alpha$  and  $\gamma$ ) and by Wagner and Birnbaum<sup>25</sup> (for  $D$ ). We will not repeat these expressions since the detailed expressions for  $\alpha$ ,  $\gamma$ , and  $D$  will certainly be different for semiconductor lasers. The dependence of these coefficients on the level populations is of importance to us, however. Since we are assuming that the two-band injection laser is similar to the two-level systems which lead to van der Pol's equation, we will assume that the populations of the conduction and valence bands play roles analogous to the level populations. Both  $\alpha$  and  $\gamma$  are linearly proportional to the difference in population between the upper and lower levels; the spectral density of the noise driving the oscillator  $D(\nu)$  is linearly proportional to the population of the upper level.

Consider the solution of Eq. (4.9) in the absence of noise, i.e.,  $N(t) = 0$ . We try a solution  $E(t) = E_0 \cos(\omega_L t)$ . If we discard the nonlinear terms at frequency  $3\omega_L$ , to which the medium may be assumed opaque, the trial solution works if

$$E_0^2 = (4/3\gamma)(\alpha - r). \quad (4.10)$$

Thus the output power of the mode is proportional to the difference between the (linear) gain and the loss in the cavity. When the field has the amplitude  $E_0$  given by (4.10), the net gain (or loss) in the mode is zero, as it must be for stable oscillation.

The presence of noise affects the oscillator in several ways. For a given population inversion the coherent output power is lowered by an amount proportional to the noise power in the mode. More serious effects are the introduction of random phase and amplitude modulation into the mode output.

Equation (4.9) has been discussed by several authors,<sup>20,21</sup> and a particularly lucid treatment has been given by Caughey.<sup>26</sup> His results are directly applicable to the present problem. We summarize his method for solving Eq. (4.9). Assume a solution of the form of Eq. (4.1) but omit the random phase of the coherent

signal, since our experiments are not sensitive to phase noise. The difficulty in the present problem comes from the nonlinear term in the gain in (4.9). Using the method of Rice,<sup>27</sup> Caughey calculates the power spectrum of  $E^3(t)$  assuming the  $E(t)$  given in (4.1). The power spectrum of  $E(t)$  is simply  $(\frac{1}{2})E_0^2\delta(\nu - \nu_L) + g^2(\nu)$ . The power spectrum of  $E^3$  contains many terms, centered about either  $\nu_L$  or  $3\nu_L$ . All of the latter are discarded. The terms centered about  $\nu_L$  are of three kinds; the first has a delta-function spectrum around  $\nu_L$  and is due to the coherent signal beating with itself three times; the second type of term represents noise with a power spectrum proportional to  $g^2(\nu)$ ; such a term comes from the beat of the coherent signal with itself and then with the noise  $e_n$ . Finally there are terms in which (a) the noise  $e_n$  beats with itself and then with the coherent signal or (b) with itself three times. These latter terms (a) and (b) are centered about  $\nu_L$  but they have noise spectra which are more spread out than  $g^2(\nu)$ . Moreover, they correspond to non-Gaussian noise.<sup>21</sup> These non-Gaussian terms must be neglected in order to proceed further; this neglect is not serious as long as the approximation  $e_n < E_0$  is valid. What follows is restricted then to an oscillator well above threshold.

Thus the power spectrum of  $E^3(t)$  is found to be

$$(3P_n + 3P_{\text{coh}})^2 g^2(\nu) + (3P_n + \frac{3}{2}P_{\text{coh}})^2 P_{\text{coh}} \delta(\nu - \nu_L). \quad (4.11)$$

As Caughey points out, this is the same as if the noise part of  $E(t)$  had been put through a linear device of gain  $3(P_n + P_{\text{coh}})$  and the sinusoidal part of  $E(t)$  through a linear device of gain  $(3P_n + \frac{3}{2}P_{\text{coh}})$ . With this picture in mind one can now write Eq. (4.9) in the form of two separated, linear equations, one homogeneous, for the sinusoidal part of the solution, the other inhomogeneous, for the noise part. These equations are

$$d^2 E_{\text{coh}}/dt^2 - \{\alpha - r - \gamma(3P_n + \frac{3}{2}P_{\text{coh}})\} dE_{\text{coh}}/dt + \omega_L^2 E_{\text{coh}} = 0, \quad (4.12)$$

$$d^2 e_n/dt^2 - \{\alpha - r - \gamma(3P_n + 3P_{\text{coh}})\} de_n/dt + \omega_L^2 e_n = (\omega_L^2/c^2)N(t).$$

The solution to the first of these is similar to (4.10) except that it now reads

$$E_0^2 = (4/3\gamma)(\alpha - r) - 4P_n. \quad (4.13)$$

This is the effect of the noise in decreasing the coherent output for given linear gain. The second equation is simply the Langevin equation for the Brownian motion of a damped harmonic oscillator.<sup>28</sup> If the driving noise is Gaussian, so is  $e_n(t)$ . Equation (4.13) can be used to eliminate  $P_{\text{coh}}$  from the second of Eqs. (4.12). The treatment of the noise properties of the linear damped harmonic oscillator driven by noise is then standard.

<sup>25</sup> W. G. Wagner and G. Birnbaum, J. Appl. Phys. **32**, 1185 (1961).

<sup>26</sup> T. K. Caughey, Trans. Am. Soc. Mech. Engrs. (Trans. ASME) **81**(3), 345 (1959).

<sup>27</sup> See *Selected Papers on Noise and Stochastic Processes*, edited by N. Wax (Dover Publications, Inc., New York, 1954), p. 276 ff.

<sup>28</sup> See Ref. 27, p. 123.



The noise power  $P_n$  and the noise bandwidth  $\Delta\nu_n$  are given as follows:

$$\begin{aligned} P_n &\propto D/P_{\text{coh}} \\ \Delta\nu_n &\propto P_{\text{coh}} \end{aligned} \quad \text{for } P_{\text{coh}} \gg P_n. \quad (4.14)$$

These are the relations between the noise properties of the mode output and the coherent signal. They show that the amplitude noise power in the mode is inversely proportional to the coherent signal, and also that the noise bandwidth is linearly proportional to the coherent power. The spectral density of the amplitude noise, in other words, decreases very rapidly with increasing strength of oscillation. (The inverse relationship between  $P_n$  and  $P_{\text{coh}}$  holds only so long as the spectral density of the driving noise  $D$  can be considered independent of the excitation level. This will be true in a limited region above threshold, where the output power is changing much more rapidly than the excitation.)

We can now return to Eq. (4.7) to describe the variation of  $\rho$  as the laser goes through threshold. Below threshold  $P_{\text{coh}}$  is zero and the expression for  $\rho$  is simply  $(\tau_n/2\tau_R)$ . The variation of  $\tau_n$  (which apart from a numerical factor is the reciprocal of the bandwidth) may be seen from the second of Eqs. (4.12). Since we are below threshold the complications due to nonlinearity are unimportant and all terms containing  $\gamma$  may be dropped. The output of the mode is narrow-band random noise with the same statistical properties as the driving noise  $N(t)$ . The noise bandwidth is  $(r-\alpha)$ . Since  $\alpha$  is proportional to the population difference, it increases with increasing excitation, and hence as threshold is approached from below the bandwidth of the noise power decreases. This means that the value of  $\rho$  detected in our intensity interferometer with its limited bandwidth will increase. This is what is observed.

Far enough above threshold for Eq. (4.2) to hold we can substitute the results of (4.14) in (4.7) and find the variation of  $\rho$  above threshold to be proportional to  $(P_{\text{coh}})^{-3}$ . This rapid decrease above threshold is also consistent with the rapid decrease actually observed. Within the experimental error of  $\pm 25\%$ , the curve for  $\rho_{11}$  in Fig. 7 varies as  $(P_{\text{coh}})^{-3}$  for values of  $J$  between 22.2 and 24.6 mA.

In the region right at threshold, where the magnitudes of  $P_{\text{coh}}$  and  $P_n$  are comparable, the approximations made in the theory break down and it becomes very difficult to find a meaningful way in which to linearize van der Pol's equation. We cannot therefore predict theoretically the magnitude of the peak in the  $\rho$ -versus- $J$  curve.

### Intensity Correlations

We have seen that the observed variation of the intensity fluctuations in a single lasing mode may be understood in terms of the response of van der Pol's oscillator to random noise. We will now show that the

observed correlations between the intensity fluctuations in different modes can be understood in terms of the response of coupled van der Pol's oscillators to random noise.

Van der Pol long ago<sup>29</sup> considered coupled circuits, but the coupling mechanism he derived for rf circuits is different from that which operates in the active medium of a laser. Although this problem is related to the case of multimode oscillation treated by Lamb,<sup>22</sup> it must always be kept in mind that the injection lasers considered here oscillate in one mode only, with the other modes producing narrow band noise. The coupling between the modes occurs via the nonlinear response of the medium to the total electric field present. For definiteness we assume three fields present at frequencies  $\omega_1$ ,  $\omega_2$ , and  $\omega_3$ ; further let us assume that it is mode 2 in which laser oscillation will occur. As in nonlinear optics we calculate the Fourier components of the total polarization<sup>23</sup>; at  $\omega_1$  the nonlinear polarization has contributions proportional to  $E_1^3$ ,  $E_2^2E_1$ ,  $E_3^2E_1$ , plus others if the modes are equally spaced in frequency. When mode 2 is oscillating, however, its field strength is considerably greater than either  $E_1$  or  $E_3$ , and the only important nonlinear terms are proportional to  $E_2^2E_1$ ,  $E_2^3$ , and  $E_2^2E_3$ , at frequencies  $\omega_1$ ,  $\omega_2$ , and  $\omega_3$ , respectively.

We can therefore write down three equations for the three fields.

$$d^2E_1/dt^2 + \{r - \alpha_1 + \gamma_1 E_2^2\} dE_1/dt + \omega_1^2 E_1 = (\omega_1^2/c^2) N_1(t), \quad (4.15a)$$

$$d^2E_2/dt^2 + \{r - \alpha_2 + \gamma_2 E_2^2\} dE_2/dt + \omega_2^2 E_2 = (\omega_2^2/c^2) N_2(t), \quad (4.15b)$$

$$d^2E_3/dt^2 + \{r - \alpha_3 + \gamma_3 E_2^2\} dE_3/dt + \omega_3^2 E_3 = (\omega_3^2/c^2) N_3(t). \quad (4.15c)$$

These are the equations which govern the fields in the three modes when the injection current is above threshold for laser oscillation in mode 2. In the approximation we are using the equation for the oscillating mode is unchanged, whereas the equations for the other modes are altered in the same way by the strong field at  $\omega_2$ .

We use these equations first to discuss the relative intensity fluctuations in the nonlasing modes. For this purpose we can replace  $E_2^2$  in the first and third equations by its time averaged value. Equations (4.15a), (4.15c) are then simply Langevin equations: The solutions  $E_1(t)$  and  $E_3(t)$  will have the character of random noise and will be Gaussian if the  $N_i(t)$  are. The bandwidth of this noise is given by the factor which multiplies  $dE/dt$ ; that is,  $(r - \alpha_{1,3})$  below threshold and by  $(r - \alpha_{1,3} + \gamma_{1,3} E_2^2)$  above threshold. Since the  $\alpha$ 's increase with increasing excitation, we see that below threshold the bandwidth of the output noise emission of the mode will decrease, and, in our detector of small bandwidth,

<sup>29</sup> B. van der Pol, Phil. Mag. 43, 700 (1922); also in *Selected Scientific Papers* (see Ref. 8).

give rise to a measured value of  $\rho$  which increases with injection level. In the nonlasing modes, however,  $(r-\alpha)$  never decreases to zero; it has some finite positive value when mode 2 goes into oscillation. The variation of the bandwidth of the nonlasing modes above threshold for mode 2 depends on the detailed form of the various  $\alpha$  and  $\gamma$  coefficients. It can be shown that the bandwidth will not decrease below a limiting value. This implies  $\rho$  in the nonlasing modes should tend to a constant value. However, it will be shown at the end of this section that there is good reason to expect the  $\rho$ 's in the nonlasing modes to fall off gradually from their highest values as the coherent power is further increased. Such behavior is actually observed in the intensity fluctuations of the nonlasing modes (see Fig. 7) and implies the bandwidth of the nonlasing modes eventually increases with increasing  $J$ .

We now use Eqs. (4.15) to explain the correlation between intensity fluctuations in different modes. We make use of the fact that  $E_2^2$  is not always equal to its time average value but rather fluctuates around it. It is clear from Eqs. (4.15a), (4.15c) that when the intensity of the lasing mode fluctuates up there is a corresponding decrease in the output of the nonlasing modes, since their gain suffers additional suppression. Similar reasoning shows that a decrease in intensity in the lasing mode should coincide with increasing intensity in the nonlasing modes. Thus the equations clearly predict the negative correlation observed between the fluctuations in the lasing and nonlasing modes.

Furthermore, since  $E_2^2$  enters all of the equations for nonlasing modes in the same way, it is clear that all nonlasing modes tend to respond in the same way to fluctuations in the intensity of mode 2; this provides the explanation of the positive correlation observed in the noise emission from separate, nonlasing modes.

We can also calculate the expected magnitude of the cross-correlation coefficient  $\rho_{12}$ . We have seen in the previous discussion that all of the nonlasing modes are influenced in the same way by the fluctuations in the lasing mode. Hence it is a reasonable physical picture to describe the fluctuations in terms of two modes only, one which is lasing and one which is not. We then assume that in the steady state the total instantaneous intensity of the two modes is constant. This is the same as assuming that the fluctuations in the two modes are

equal and opposite. With this assumption one can show very readily that  $\rho_{12} = -\rho_{11}(P_1/P_2) = -\rho_{22}(P_2/P_1)$ . Despite the greatly simplified model used to derive these relations they reproduce within 30% the measured  $\rho_{12}$ -versus- $J$  curve above threshold. At or below threshold they should not be expected to apply since in this region the lasing mode is not strong enough to dominate the other modes.

The equations in the last paragraph can be used to explain the bending over of the curve of  $\rho_{22}$ -versus- $J$  which is evident in Fig. 7. These relations clearly imply  $\rho_{22} = \rho_{11}(P_1/P_2)^2$ ; furthermore, we know that well above threshold  $\rho_{11}$  varies as  $P_1^{-3}$ , and  $P_2$  saturates at a constant value. Under these conditions  $\rho_{22}$  varies as  $P_1^{-1}$  which is consistent with  $\rho_{22}$  versus  $J$  in Fig. 7. This result depends on a two-mode model; this model is fairly good for the diode of Fig. 7 since the power in the third strongest mode is down considerably from the second strongest.

## V. CONCLUSION

Using two independent methods, which give quantitative agreement, we have measured the intensity fluctuations in the lasing mode and in the nonlasing modes of cw GaAs lasers. We have observed the change in the noise properties of the lasing mode as it passes through the threshold region. We have observed the output of the nonlasing modes to be narrow-band Gaussian random noise at currents above threshold, where the lasing mode has quieted and is best described by an amplitude-stabilized field plus a weaker noise field. We have shown that all of the observations are consistent with the description of the lasing mode as a van der Pol oscillator. And finally we have seen that the observed mode coupling is consistent with the description of the several modes as coupled nonlinear oscillators.

## ACKNOWLEDGMENTS

The authors are grateful to R. F. Rutz and R. C. McGibbon for supplying the lasers used in this work. We wish to acknowledge useful conversations with Dr. M. I. Nathan, Dr. N. S. Shiren, and Professor L. Mandel. We wish to thank Dr. G. J. Lasher for useful conversations and for comments on the manuscript.